

Light Lanthanides Determination by Fast Fourier Transform Continuous Cyclic Voltammetry after Separation by Ion-exchange Chromatography

Mohammad Reza Pourjavid,¹ Parviz Norouzi^{*1,2}, Mohammad Reza Ganjali^{1,2}

¹Center of Excellence in Electrochemistry, Faculty of Chemistry, University of Tehran, Tehran, Iran

²Endocrinology & Metabolism Research Center, Medical Sciences/University of Tehran, Tehran, Iran

*E-mail: Norouzi@khayam.ut.ac.ir

Received: 25 May 2009 / Accepted: 20 June 2009 / Published: 19 July 2009

Cation-exchange separations of the light lanthanides (La^{3+} , Ce^{3+} , Pr^{3+} and Nd^{3+}) on Nucleosil 100-5-SA ion-exchange column with use of α -hydroxyisobutyric acid (HIBA) as elution agent was investigated in this study. For easy detection and identification, fast Fourier transform continuous cyclic voltammetry (FFT-CCV) was used as detection method. The developed technique is very simple, precise, accurate, time saving, and economical, compared to previously reported methods. The influence of HIBA concentration as well as pH of eluent was studied. The best performance obtained at pH value of 4.0, scan rate value of 30 V/s, accumulation potential of -300 mV, and accumulation time of 0.3 s. The proposed method displays a linear dynamic range between 250 and 21000 ppb and a detection limit of 90 ppb. Precision, inter-day precision and accuracy of the assay have presented too. This method posse some advantages in comparison with former ones such as, no need for the removal of oxygen from the test solution, a reasonable detection limit, and finally the method is sufficiently fast for the determination of any such compound, in a wide variety of chromatographic methods. The potential waveform, consisting of the potential steps for cleaning, accumulation and potential ramp of analyte, was continuously applied on an Au disk microelectrode (12.5 mm in radius).

Keywords: Light lanthanides; α -hydroxyisobutyric acid; Flow injection; Continuous cyclic voltammetry

1. INTRODUCTION

Lanthanides are separated from other elements in a mineral by precipitation with a suitable reagent, but as they occur together, their physico-chemical properties are similar and their separation from each other by ordinary chemical means is difficult and expensive process [1]. There are many reports in use of analytical separation methods such as high performance liquid chromatography

(HPLC), ion chromatography (IC) and capillary electrophoresis (CE) for separation of lanthanides [2-14]. They have been shown to be rapid, precise, accurate, and low-cost for the determination of lanthanides in a wide variety of matrices. Separation is based mainly on the exploitation of the metal complexation properties of the lanthanides. These complexation reactions can take place in either the mobile or stationary phase and even in both. Researchers suggested different chromatographic mechanisms account for the complexation reactions mentioned above such as reversed-phase [11, 15], ion-pair [16, 17], ion-exchange [18–21] or chelating ion chromatography (HPCIC) [22, 23].

Ion chromatography is an attractive procedure for lanthanides analysis. Typically, low-capacity cation-exchange resins are used as stationary phases, with aqueous solutions of complexing agents as the mobile phases. Many eluents like α -hydroxyisobutyric acid (α -HIBA) [24-30], mandelic acid [29], oxalic acid [15], glycolic acid [30], lactic acid [31] can use for separation of lanthanide ions. Except of these carboxylic acids, EDTA used as mobile phase recently for separation of lanthanides [32]. Of course a mixed gradient of two eluents can be used too [33, 34]. HIBA is the most popular eluting agent amongst different hydroxycarboxylic acids that used for the separation of lanthanides and has been shown to provide a good degree of separation between adjacent lanthanides in ion chromatography. Lanthanide metal ions form singly positive charged complexes with HIBA that lower the affinity of the lanthanide for the cation-exchange resin. The degree of complexation increases with increasing atomic number of elements. Two equilibria must be considered. The first one is the equilibrium between the eluent and the resin, and the second one is the equilibrium between the lanthanide and the lanthanide-HIBA complexes. This secondary equilibrium permits the separation of the lanthanides because each lanthanide has a different relative stability with HIBA. Therefore, lanthanides that form the most stable complex with HIBA, such as Neodymium, will spend relatively more time in the eluent and elute first. Lanthanides such as lanthanum, which forms a weaker complex with HIBA, prefer to spend more time in the resin and elute later. Stronger complexing agents such as oxalic acid cause to formation of anionic complexes. In these cases, anion-exchange chromatography uses for separation. Because the strongest complexes are the most negatively charged, the elution order is reversed from that of the cation-exchange separations. So, in the present study we used HIBA as eluting agent.

The separated lanthanides are occasionally determined using the post-column derivatization method. Different complexing reagents especially Arsenazo-III and PAR have been proposed for achieving an efficient detection for all lanthanides, and also for suppressing interference problems due to the presence of other cations [1, 4, 5, 9]. Use of ICP-AES and ICP-MS interfaced with ion chromatography for detection of lanthanides ever-increasing in the last years [35-37]. A large amount of organic reagent used as the mobile phase may cause spectral interferences due to molecular bands such as CO, CN, OH or NH. In addition, due to the high viscosity of concentrated salt solutions, they tend to influence the nebulization efficiency. In the case of ICP-MS, the interferences due to polyatomic ions cause a serious problem [38, 39].

Potentiometric sensors can offer an inexpensive and convenient analysis method of rare-earth ions in solution, provided that acceptable sensitivity and selectivity are achieved. There are many reports about ion selective electrodes (ISEs) for lanthanide ions in last decade [40-52]. This paper gives the results of an investigation on the application of fast Fourier transform continuous cyclic

voltammetric (FFT-CCV) method for determination of light lanthanides (La, Ce, Pr and Nd). Detect of lanthanide ions with FFT-CCV is faster than other detection method, especially UV-Vis spectrometry, because in these methods pre- or post-column derivatization is necessary that can be time consuming and expensive.

Because of the selective detector, voltammetric techniques are useful for the samples. In addition, owing to the movement of the analyte zone in an electrochemical flow cell for flowing solutions, the application of these techniques requires fast analyte accumulation and fast potential sweeping (which is not appropriate for large electrodes) [53, 54]. The use of voltammetric techniques have been further stimulated by the advent of ultra-micro electrodes (UMEs), due to their steady state currents, higher sensitivity, increased mass transport and their ability to be used in electroanalysis in solutions with high resistance [55, 56]. UMEs, for instance, have been applied as sensors in various techniques such as flow injection analysis (FIA) [57, 58], cardiovascular monitoring and organic compounds analysis [59, 60]. Another problem comes from the changes in the characteristics of the electrode surface during the potential scan. The electrode signal will have a large background current, if the surface of the solid electrode is oxidized and reduced during voltammetric measurements (the response of the electrode will have a large background current), which is associated with high levels of noise due to the structural changes of the electrode surface, currents like this can interfere with the electrode processes of interest, and may adversely affect the detection limits of the methods used.

The background current in voltammetric measurements, as discussed later, can provide useful information about the adsorption processes and changes in the double layer at the electrode surface [61]. In addition, small amounts of adsorption of species, present in the solution, on the electrode surface can strongly affect the cathodic and anodic currents of red/ox reaction of the electrode. For calculation of the signal of the analyte and noise reduction, a special computer based numerical method is also introduced. The calculation of signal was based on the net partial and total charge exchanges at electrode surface and was done by integrating the currents at the selected potential range at the cyclic voltammogram (CV). Depending on the conditions applied, the detector can be used in determination of various species in chromatographic analysis methods (e.g., HPLC and IC). Moreover, the sensitivity of the method significantly depends on the mode of data processing that is used in calculation of the detector response.

2. EXPERIMENTAL PART

2.1. Apparatus

The model IC760 (Metrohm) was used during the ion chromatographic experiments. Characterization of some useful cation exchangers was presented in Table 1 [62]. However, in the case of separation of the light lanthanides, the ion-exchanger DOWEX 50WX8 was used. The operation was completed under the flow rate 1.5 mL/min.

A 10-roller peristaltic pump (UltrateckLabs Co., Iran) and a four-way injection valve (Supelco Rheodyne Model 5020) with a 50- μ L sample injection loop consisted of the necessary equipment for

the flow injection analysis. Flow rate of the pump was set at 3mL/min during an experimental run. The solutions were introduced into the sample loop by a plastic syringe. After, opening the loop in the way of eluent flow, the sample can pass over the working electrode. In figure 1, the electrochemical cell of the flow injection analysis was shown in detail. The potentiostat applies a potential in the range of gold oxidation in acidic media and the potential waveform was shown in figure 2. The special program on computer can monitor the cyclic voltammograms online and every change on current or charge will be shown in program.

Table 1. Characterization of cation-exchanger

Character (*)	Trade Name	Procedure (**)	Active Group	Matrix	Effective pH	Total Exchange Capacity (meq/ml)	Standard Mesh Range
SAC	Dowex 50	1	Sulfonic acid	Polystyrene	0-14	Na ⁺ 1.9 H ⁺ 1.7	20-50 (wet)
SAC	Dowex MPC-1	4	Sulfonic acid	Polystyrene	0-14	1.6-1.8 H ⁺ form	20-40 (wet)
SAC	Dowex 50WX8	1	Sulfonic acid	Polystyrene	0-14	1.7 H ⁺ form	50-100
SAC	Duolite C-20	2	Sulfonic acid	Polystyrene	0-14	2.2	16-50
SAC	Ionac 240	3	Sulfonic acid	Polystyrene	0-14	1.9	16-50
SAC	Duolite C-3	2	Methylene Sulfonic	Phenolic	0-9	1.1	16-50
WAC	Dowex CCR-1	4	Carboxylic	Phenolic	0-9	-	20-50 (wet)
WAC	Duolite ES-63	2	Phosphonic	Polystyrene	4-14	3.3	16-50
WAC	Duolite ES-80	2	Aliphatic	Acrylic	6-14	3.5	16-50

* SAC: Strong Acid Cation, WAC: Weak Acid Cation

** 1. Dow, 2. Diamond Shamrock, 3. Ionac, 4. Nalco

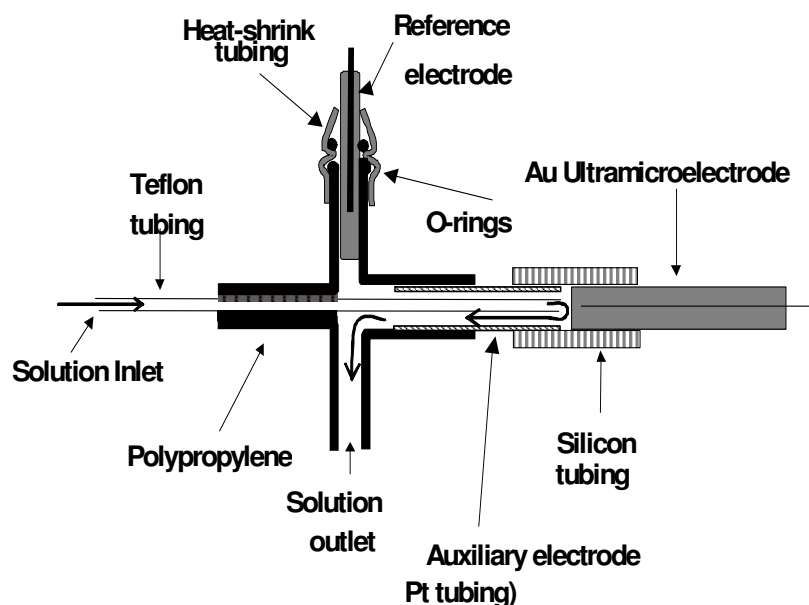


Figure 1. Diagram of the electrochemical cell

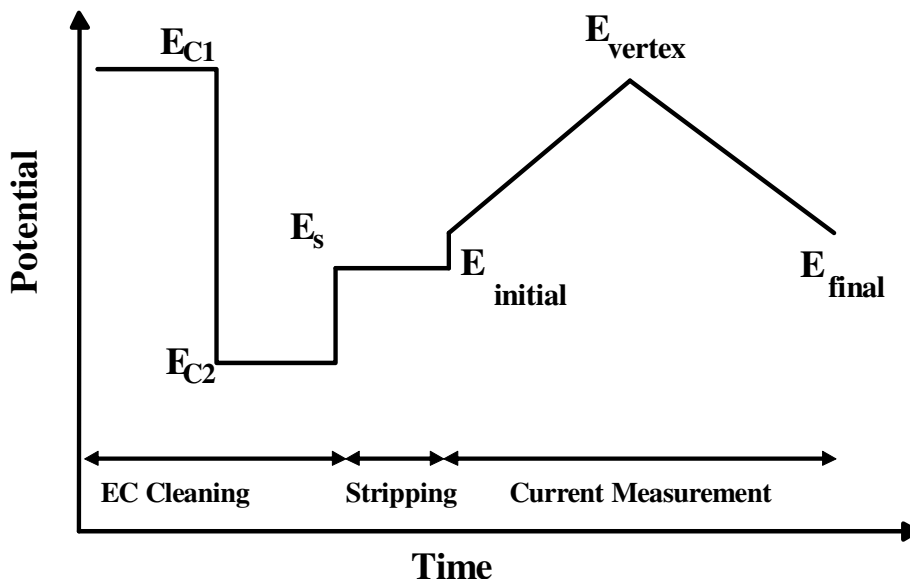


Figure 2. The diagram of the applied potential waveform

2.2. Reagents

The oxide of lanthanides, hydrochloric acid and HIBA were of the high purity available from the Merck Chemicals and were used without further purification. HIBA was 0.3 M buffered at pH 4.0 with sodium hydroxide. The reagents for the preparation of the eluent solution for the flow injection analysis (0.05 mol/L H_3PO_4) and 1 mol/L NaOH (for the pH eluent adjustment), were obtained from Merck. All solutions were prepared in doubly distilled deionized water, filled with the background electrolyte solution and they were used without the removal of the dissolved oxygen.

2.3. Background electrolyte (BGE) and standard solutions

The running buffer or BGE was made by phosphoric acid (85%, w/v) with the addition of 8.7mL into a 1000mL volumetric flask and dilution to a constant volume with distilled water. The pH was adjusted to the value of 4.0 with sodium hydroxide. The solutions were freshly prepared and filtered, using a Millipore filter (0.45 μm) each day.

For the preparation of the standard stock solutions, pure lanthanide oxides dissolve in 0.36 M hydrochloric acid. These solutions were diluted with doubly distilled deionized water to about 10 ppm of metal. Also, for the preparation of the standard solutions for FIA, aliquots of the standard stock lanthanides solution were dispensed into 10mL volumetric flasks. These flasks were filled up with the running buffer to give final concentrations range of 10 – 21000 ppb.

2.4. Electrode preparation

The construction of the gold UMEs (12.5 μm in radius) involved the metal micro-wires (Good fellow Metals Ltd., UK) sealing into a soft glass capillary. Then, the capillary was cut perpendicularly to its length to expose the wire. Silver epoxy (Johnson Matthey Ltd., UK) was used for the electrical contacts. Previous to the initiation of any experiment, the electrode surface was polished for 1 min using extra fine carborundum paper and, afterwards, for 10 min with 0.3 μm alumina. Prior to being placed in the cell, the electrode was washed with water. In all measurements, an Ag (s)|AgCl (s)|KCl (aq, 1 M) reference electrode was used. The auxiliary electrode was made of a Pt wire, 1 cm in length and 0.5 mm in diameter.

3. RESULTS AND DISCUSSION

3.1. Data acquisition and processing

For the data acquisition, a setup of a PC PIV Pentium 900MHz microcomputer, equipped with a data acquisition board (PCL-818HG, Advantech. Co.) and a custom made potentiostat, was used. All data acquisition and data processing programs were developed in Delphi 6[®] program environment. In figure 2, the applied waveform potential diagram during the cyclic voltammetric measurements is shown. The potential waveform consists of three parts; (a) Potential steps, E_{c1} and E_{c2} (which are used for the oxidation and reduction of the electrode surface, respectively), during which the electrochemical cleaning of the electrode surface takes place, (b) E_c , where the analyte accumulation takes place and (c) the potential ramp, where the current measurements occur.

During the scan, some of the adsorbed analyte molecules are desorbed. Depending on the rate of those processes and the scan rate, the amount of the desorption analyte molecules (during the scan) can be changed. The important point here is that part of the adsorbed analyte molecules still remain on the electrode surface, inhibiting the red/ox process of the electrode surface. In this technique, ΔQ is calculated according with the all current changes at the CVs [63-67].

Application of a special digital filtration, which is applied during the measurement, is one of the considerable aspects of this method. At first, an electrode CV was recorded and then by applying FFT on the collected data, the existing high frequency noises were indicated. With the aid of this information, the cutoff frequency of the analog filter was set at a certain value (where the noises were removed from the CV).

Since the crystal structure of a polycrystalline gold electrode is greatly affected by the condition of the applied potential waveform [56], different potential waveforms were examined in order to obtain a reproducible electrode surface (or a stable background signal). In fact, the application of cyclic voltammetry for the determination of electroactive compounds mainly faces low stability of the background signal, due to the changes taking place in the surface crystal structure during the oxidation and reduction of the electrode in each potential cycle. The electrochemical oxidation process of the gold surface starts with the hydroxyl ion electrosorption, which at more positive potentials results in the gold oxide formation, undergoing structural rearrangement [68].

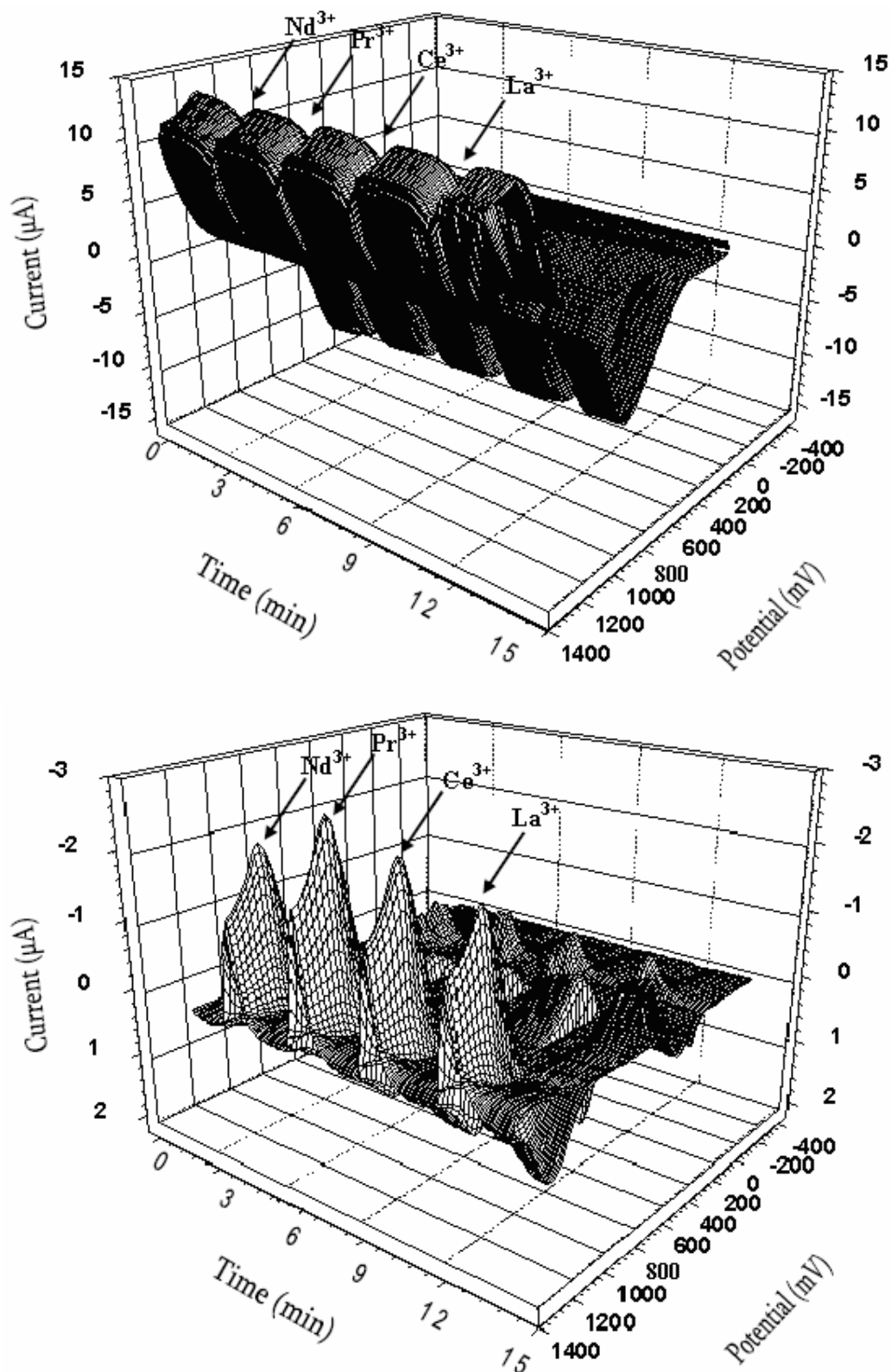


Figure 3. (a) Cyclic voltammogram at a $12.5 \mu\text{m}$ Au ultramicroelectrode recorded during a flow injection experiment. The eluent was $0.05 \text{ M H}_3\text{PO}_4$, the flow rate was $100 \mu\text{L/s}$ and the sweep rate was 30 V/s . Each scan was preceded by 100 ms (at 600 mV) and 100 ms (at -800 mV) conditioning, respectively. The accumulation time was 300 ms at -300 mV . The injected solution ($50 \mu\text{L}$) contained 1.0 ppm La^{3+} , Ce^{3+} , Pr^{3+} and Nd^{3+} in $0.05 \text{ M H}_3\text{PO}_4$. (b) Curves result from the subtraction of the CVs average (in the absence of the analytes) from the test of the CVs in (a).

An example of the recorded CVs is demonstrated in figure 3 (a and b). Figure 3a shows a CV sequence recorded during the flow analysis for the lanthanides determination. The injection volume was 50 μL of (1.0 ppm) La^{3+} , Ce^{3+} , Pr^{3+} and Nd^{3+} (in 0.05 mol/L H_3PO_4) into the eluent solution, containing 0.05 mol/L H_3PO_4 . The time axis of the graph represents the time of the flow injection experiment. In the absence of light lanthanide ions, the shape of the CV curves is typical for a polycrystalline gold electrode in acidic media [69]. Figure 3b illustrates the absolute current changes in the CVs curves, after subtracting the average background of 4 CVs (in the absence of the analytes). Evidently, this way of presenting the electrode response gives more details about the adsorbed ion effect on the CV currents. As a matter of fact, the curves show that the current changes mainly take place at the potential regions of the oxidation and reduction of gold. When the electrode-solution interface is exposed to light lanthanide ions, which can be adsorbed on the electrode, the oxide formation process becomes severely inhibited. In detail, the surface process inhibition causes significant change in the currents at the potential region and, as a consequence, the profound changes in the shape of the CVs take place.

Theoretically, the analyte response can be affected by the thermodynamic and kinetic parameters of adsorption, the mass transport rate and the electrochemical behavior of the adsorbed species. The free energy and the adsorption rate depend on the electrode potential, the electrode material and, to some extent, on the choice of the concentration and the type of the supporting electrolyte. By taking these points into consideration, for the achievement of the detector maximum performance, the effect of the experimental parameters (such as the pH of the supporting electrolyte, the potential, the accumulation time and the potential scan rate) must be examined and optimized [70-76].

Table 2. Stability constants ($\log K$) of light lanthanides with α -HIBA used as complexing agent at 20°C

Lanthanide	$\log K$
Lanthanum	5.53
Cerium	5.95
Praseodymium	6.21
Neodymium	6.30

3.2. Experimental parameter optimization

Stability constants of the Ln-eluent complexes affect the elution pattern of lanthanides. If the stability constant of Ln-eluent complex be more, it's elution will be faster and of course the less stability constant of complex, the slower will be it's elution. Generally for all the eluents, the stability constant increase from La to Lu and this explain the elution pattern in the order of decreasing atomic number from Lu to La in the cation-exchanger. The nature of metal ion and eluent as well as the environmental factors such as solvent or medium, concentration, temperature and pressure can affect

the formation of a complex between them [77]. Hence the stability constants for a given metal-eluent complex under different environmental conditions can be different. The log values of the stability constant for complexes of light lanthanides with HIBA vary from 5.53 for La (III) to 6.30 for Nd (III) that reported in the literature [78] are given in Table 2. These give only a qualitative picture of the behavior during separation of lanthanides; however the exact performance can be different.

3.2.1. Effect of pH of eluent on retention of lanthanide ions

Effect of mobile phase pH on the elution pattern of a mixture of light lanthanide ions using HIBA is shown in figure 4. This effect was monitored using retention factor (K). The analytical expression for K is:

$$K = \frac{(t_R - t_0)}{t_0} \quad (1)$$

In this equation t_0 is retention time of non-retained peak and t_R is retention time of the eluent retained. As can be seen, increasing pH from 3.0 to 6.0 caused decrease of retention factor (K) for lanthanide ions. The elution efficiency of carboxylic acids changes with pH. This factor of the carboxylic acid depends on its strength, which in turn depends on its pH. The α -hydroxycarboxylic acids tested were all weak acids and undergo only partial ionization and hence show poor eluting strength at low pH [15]. With increasing pH, the elution efficiency increased due to greater ionization of the $-\text{COOH}$ group. Against the low pH, at higher pH, the retention factors for different lanthanides are quite close. So, pH 4.0 was selected as the optimum pH, which gives adequate resolution in a shorter time. Furthermore this pH was chosen because it is near to that of the maximum buffer capacity for HIBA.

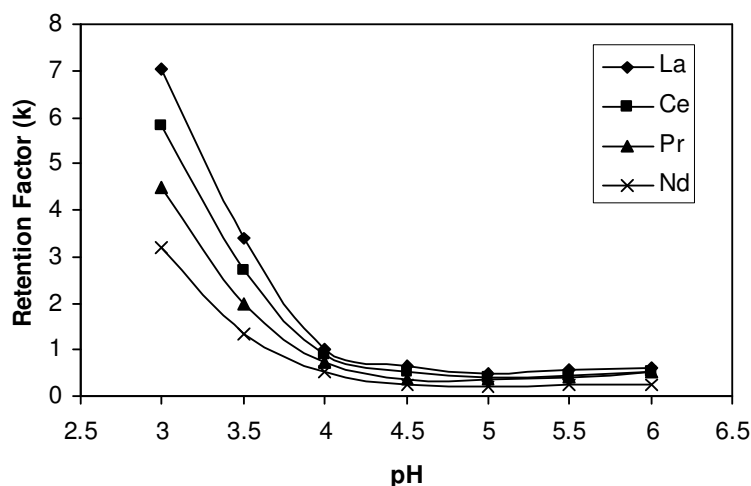


Figure 4. Effect of pH of mobile phase on retention of light lanthanides DOWEX 50WX8 under isocratic condition: 0.3 M of HIBA

3.2.2. Effect of concentration of eluent on retention of lanthanide ions

The influence of the concentration of HIBA on retention of light lanthanides is shown in figure 5. In high concentrations of eluent, elution of lanthanides is faster. The effect of concentration of HIBA was studied at pH 4.0. Under this condition, HIBA is ~ 63% ionized ($pK_a = 3.77$) [79]. With the increase in concentration of α -HIBA, the concentration of α -hydroxyisobutyrate ions increases in the mobile phase and this results in faster elution of lanthanides on the column.

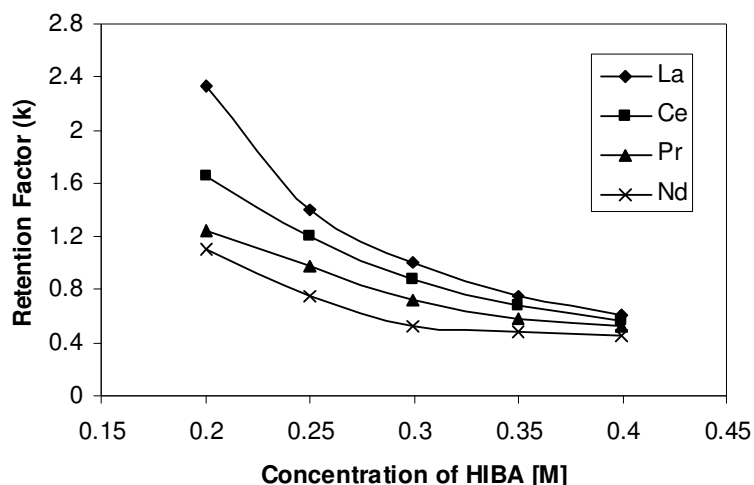


Figure 5. Effect of concentration of HIBA of pH 4.0 on retention of lanthanides on DOWEX 50WX8

3.2.3. Influence of sweep rate, accumulation potential and accumulation time

For the investigation of the scan rates influence and the eluent flow rate on the sensitivity of the detector response, solutions having a concentration of (1.0 ppm) in La^{3+} , Ce^{3+} , Pr^{3+} and Nd^{3+} were injected. At different scan rates (from 5 to 100 V/s) and eluent flow, the detector responses to the injected sample were recorded. These results are presented in figure 6. As it is clear from figure 6a, the detector exhibits the maximum sensitivity at the scan rate of (30 V/s) and figure 6b shows that flow rate of (3 mL/min) is the best. The sweep rate effects on the detection performance can be considered in three different aspects: firstly, speed in data acquisition; secondly, kinetic factors of the lanthanide ions adsorption and, finally, the eluent flow rate which controls the time window of the solution zone in the detector. The main reason for the application of high scan rates is prevention from desorption of the adsorbed lanthanide ions during the potential scanning (because under this condition, the inhibition outcome of the adsorbed lanthanide ions on the oxidation process can take place).

It is a fact that the employment of high scan rates is required for the use of this detection method in conjunction with fast separation techniques such as capillary electrophoresis. From this point of view, it is necessary to check how the method sensitivity is affected by the sweep rate. Therefore, high sweep rates must be employed to detect the amount of the adsorbed analyte on the electrode surface, so that the potential scanning step is short in comparison with the accumulation

period. An important point to be taken into consideration is the time when the lanthanide ions accumulation occurs at a potential that is greater or smaller than E_i . However, the sensitivity of the detection system mainly depends on the potential sweep rate, mostly because of the adsorption kinetic factors and the instrumental limitations. Notably, any changes in the parameters, related to the adsorption process and affecting the applied potential, the time and the potential of accumulation, severely influence the sensitivity of the measurement. For that reason, the influence of the accumulation potential and time on the response of the method for the injection of a solution of (1.0 ppm) La^{3+} , Ce^{3+} , Pr^{3+} and Nd^{3+} in 0.05 mol/L H_3PO_4 , was studied. Figure 7 shows the detector response over the accumulation potential ranges from (-800 to 600 mV) and the accumulation time range from (0.05 to 1.0 s). From figure 7a and 7b derives the conclusion that the optimum conditions to be chosen are accumulation potential of (-300 mV) and accumulation time of (300 ms), on the grounds that the electrode surface becomes lanthanide ions saturated within a (1300 ms) time window.

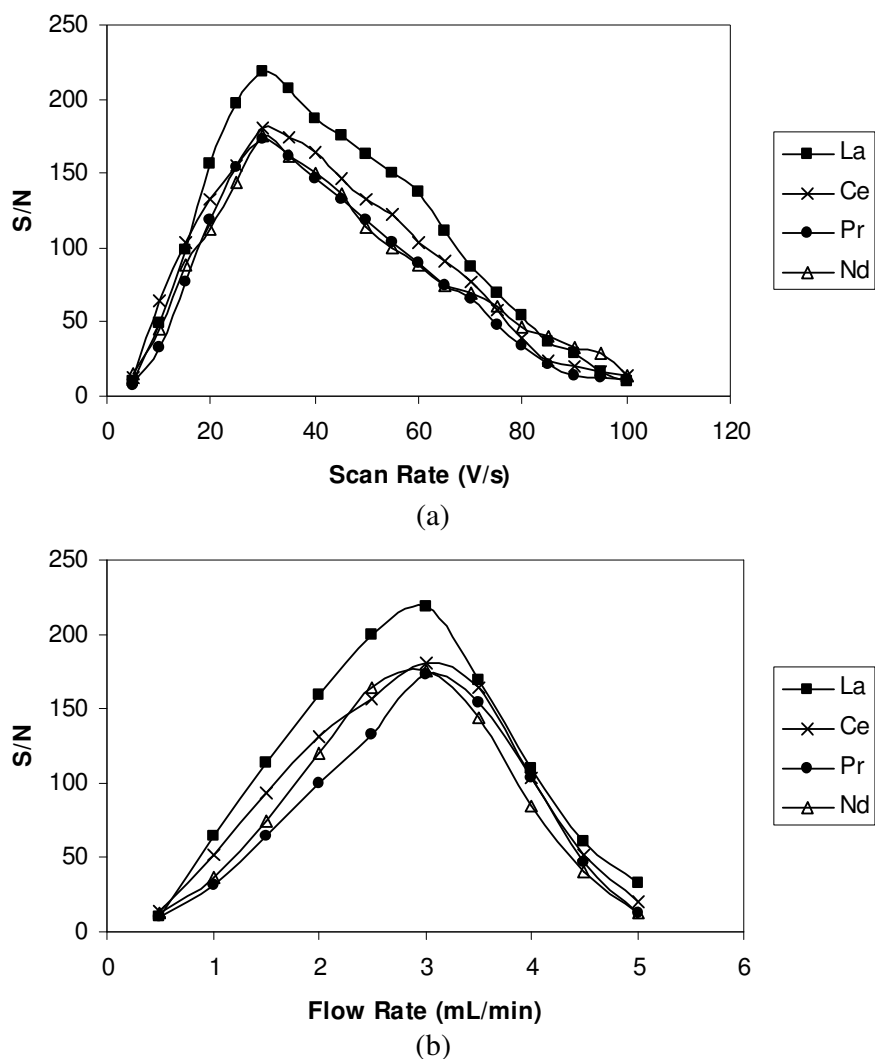
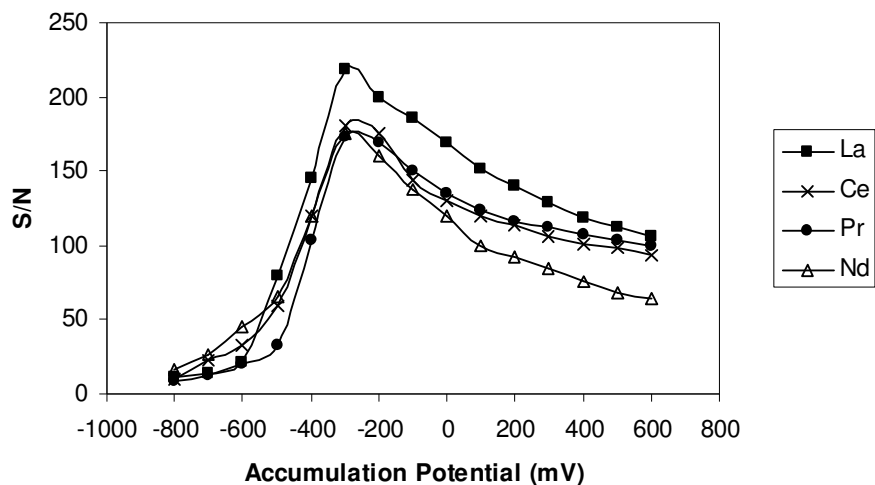
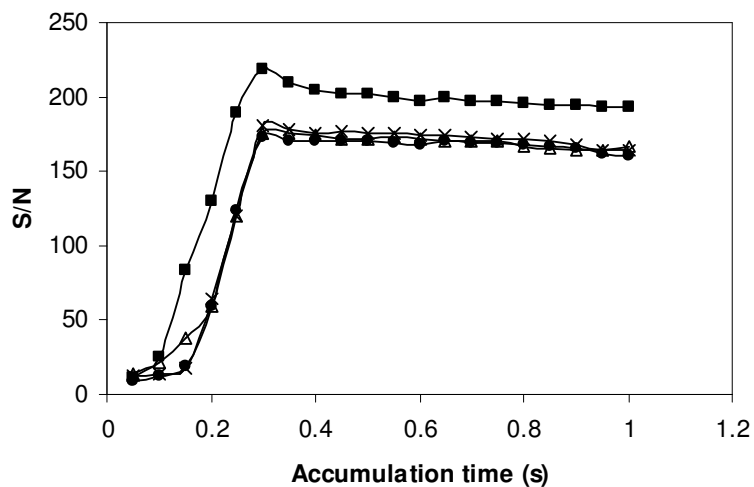


Figure 6. (a) The effect of the sweep rate and (b) the effect of flow rate on the response of the Au electrode (with a radius of $12.5\mu\text{m}$) to injections of 1.0 ppm La^{3+} , Ce^{3+} , Pr^{3+} and Nd^{3+} in 0.05 mol/L H_3PO_4 .

On the electrode, the lanthanide ions accumulation takes place during the accumulation step (assuming that an appropriate potential is selected). In fact, the difference in the saturation time of the various compounds can be related to the existing differences in their kinetics of the electron transfer and mass transport. As mentioned above, the surface of the gold ultra microelectrode is small and in a short time the electrode surface can be saturated.



(a)

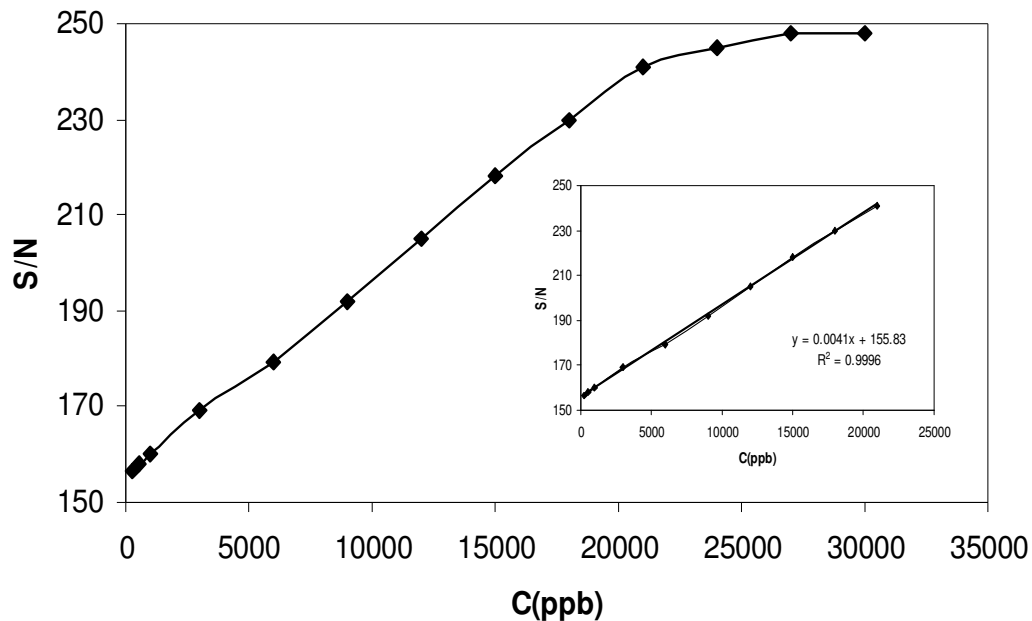


(b)

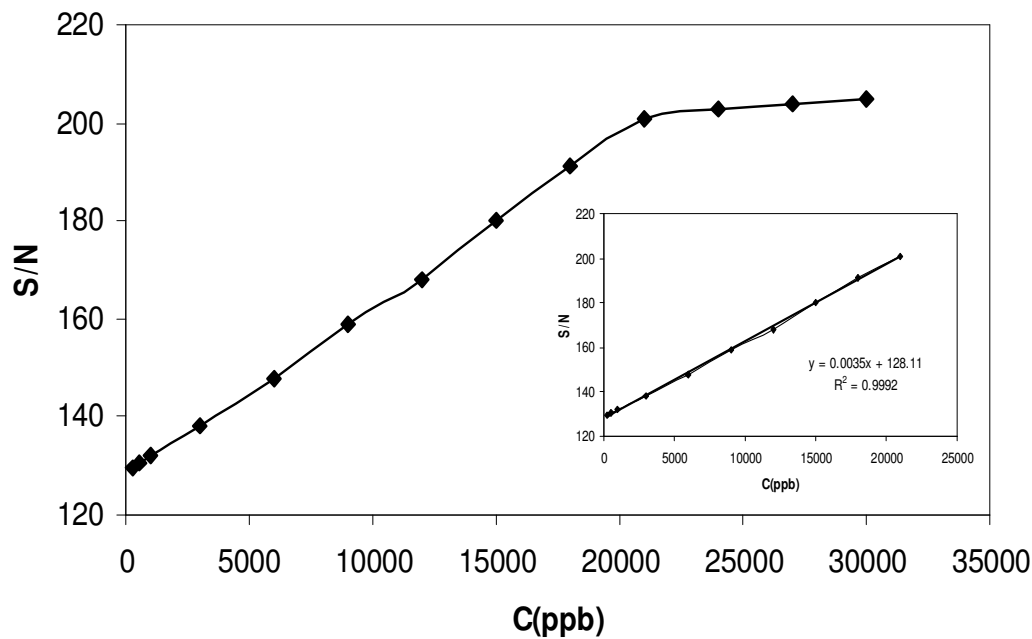
Figure 7. (a) The effect of the accumulation potential and (b) the effect of the accumulation time on the electrode response to injections of 1.0 ppm La^{3+} , Ce^{3+} , Pr^{3+} and Nd^{3+} in 0.05 mol/L H_3PO_4 .

3.3. Validation

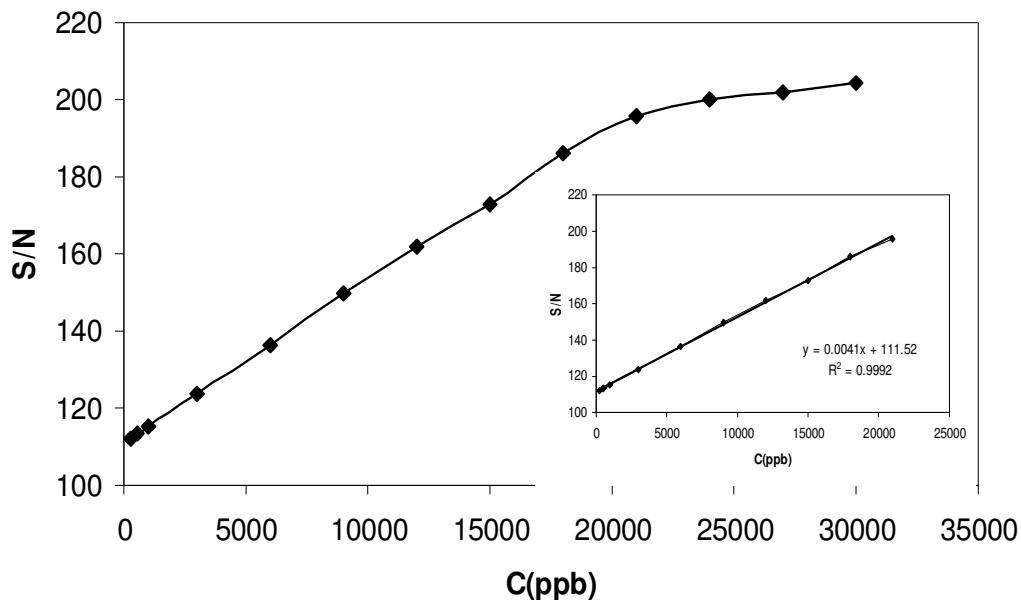
The method was validated in terms of linearity, limit of quantitation (LOQ), limit of detection (LOD), precision, accuracy, ruggedness/robustness, recovery and selectivity [80-83].



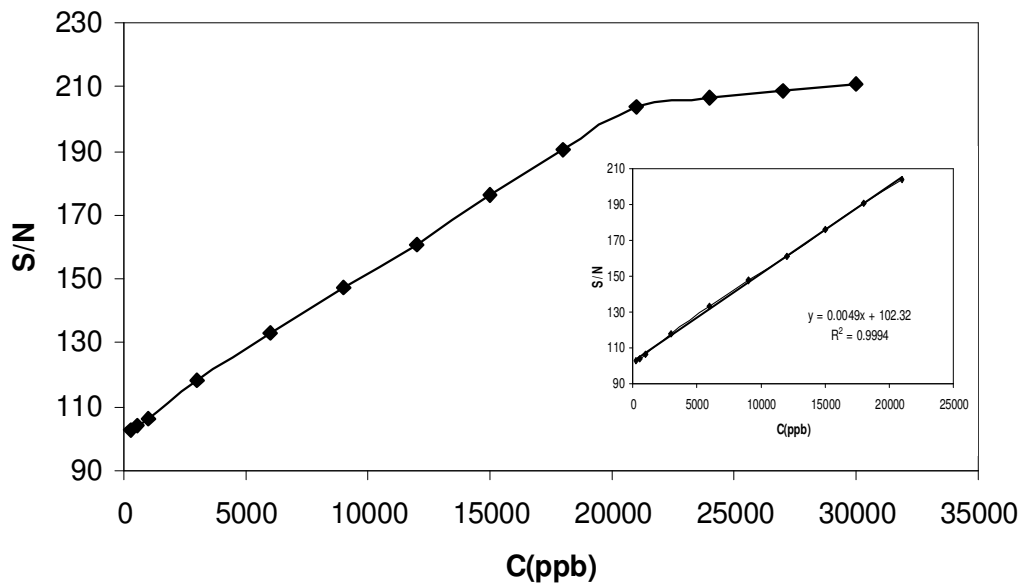
(a)



(b)



(c)



(d)

Figure 8. Calibration curves obtained for (a) La³⁺, (b) Ce³⁺, (c) Pr³⁺, (d) Nd³⁺ ions on the Au electrode in 0.05 mol/L H₃PO₄.

The linearity was evaluated by linear regression analysis, which was calculated by the least square regression method [84, 85]. The calibration curves, constructed for light lanthanide ions were linear over the concentration range of (250–21000 ppb). The peak areas of La^{3+} , Ce^{3+} , Pr^{3+} and Nd^{3+} were plotted versus its concentration and, then, linear regression analysis was carried out on the resultant curve. After this analysis, a correlation coefficient of $R = 0.999$ and %R.S.D. values, ranging from 0.18 to 3.85 % across the studied concentration range, were obtained. Typically, the regression equation for the calibration curve was found to be $Y = 0.0041X + 155.83$, $Y = 0.0035X + 128.11$, $Y = 0.0041X + 111.52$ and $Y = 0.0049X + 102.32$ for La^{3+} , Ce^{3+} , Pr^{3+} and Nd^{3+} respectively. Figure 8 depicts the calibration graphs that resulted from the monitoring of these lanthanide ions in a 0.05 mol/L H_3PO_4 .

Concerning the LOD value, it was measured as the lowest analyte amount that may be detected to produce a response, which is significantly different from that of a blank one. The limit of detection was approved by calculations, based on the standard deviation of the response (δ) and the slope (S) of the calibration curve, at the levels approaching the limits according to the equation $\text{LOD} = 3.3 (\delta/S)$ [86]. The LOD for La^{3+} , Ce^{3+} , Pr^{3+} and Nd^{3+} was found to be 90 ppb. On the other hand, the LOQ was measured as the lowest analyte amount that can be reproducibly quantified above the baseline noise, for which triplicated injections resulted in an R.S.D. ≤ 1.49 %. A practical LOQ, giving a good precision and acceptable accuracy, was equivalent to 250 ppb.

The precision of the assay was investigated with respect to both repeatability and reproducibility. The repeatability was investigated by injecting nine replicate samples of each of the (250, 10000 and 21000 ppb) standards. Additionally, the inter-day precision was assessed by injecting the same three concentrations over 3 consecutive days. The results are written in Table 3.

Table 3. Precision and inter-day precision of the assay

	Standard Solutions (ppb)	Precision		Inter-day Precision	
		Mean Concentration (ppb)	RSD (%)	Mean Concentration (ppb)	RSD (%)
La^{3+}	250	253	3.19	254	3.51
	10000	10037	2.32	10039	2.52
	21000	20888	1.12	20886	1.00
Ce^{3+}	250	252	3.25	254	3.60
	10000	10025	2.73	10036	3.00
	21000	20883	0.83	20867	1.15
Pr^{3+}	250	251	3.32	253	3.78
	10000	10043	2.50	10053	3.21
	21000	20884	0.87	20882	1.53
Nd^{3+}	250	260	2.80	255	3.51
	10000	10011	1.99	10016	2.52
	21000	20968	1.17	20960	1.53

Regarding the accuracy of the assay, it was determined by the interpolation of replicate ($n = 6$) peak areas of three accuracy standards (250, 10000 and 21000 ppb) from a calibration curve prepared

as previously described. In each case, the relevant error percentage and the accuracy were calculated. Table 4 shows the resultant concentrations with their relevant error percentage.

Table 4. Accuracy of the assay

	Standard Solutions (ppb)	Resultant Concentration (ppb)	Relevant Error (%)
La ³⁺	250	256 ± 2.04	2.40
	10000	10098 ± 63.22	0.98
	21000	20899 ± 73.50	.48
Ce ³⁺	250	258 ± 4.65	3.20
	10000	10111 ± 42.55	1.11
	21000	20908 ± 66.66	0.44
Pr ³⁺	250	254 ± 3.12	1.60
	10000	10067 ± 25.01	0.67
	21000	20942 ± 51.36	0.28
Nd ³⁺	250	259 ± 5.50	3.60
	10000	10085 ± 60.27	0.85
	21000	20921 ± 24.17	0.38

Table 5. Influence of the changes in the experimental conditions on the performance of the FIA system

Parameter	Modification	%Recovery			
		La ³⁺	Ce ³⁺	Pr ³⁺	Nd ³⁺
pH	3.9	100.6	99.9	100.2	99.6
	4.0	100.6	100.3	100.5	100.0
	4.1	99.8	100.2	100.4	99.8
Flow Rate (mL/min)	2.6	100.0	100.4	98.8	100.0
	2.8	100.2	100.3	100.6	100.0
	3.0	100.1	100.3	99.8	100.2
Buffer	0.07	98.7	101.3	100.3	100.3
Composition (M)	0.06	99.9	102.0	101.7	102.0
	0.05	100.1	100.0	100.0	99.1
Lab.	20	101.1	99.4	101.8	100.0
Temperature (°C)	25	101.2	101.5	101.6	101.4
	30	101.1	101.2	99.7	101.4

The ruggedness of the method was calculated by the comparison of the intra- and inter-day assay results for lanthanide ions undertaken by two analysts. The %R.S.D. values for intra- and inter-day assays of lanthanide ions in the cited formulations, performed in the same laboratory by the two analysts, did not exceed 4 %; thus, indicating the ruggedness of the method. Also, the robustness of the method was investigated under a variety of conditions such as small changes in the pH of the eluent, in

the flow rate, in the buffer composition and in the laboratory temperature [87]. As it can be seen in Table 5, the light lanthanide ions recovery percentages were good under most conditions, not demonstrating any significant change when the critical parameters were modified.

3.4. Sensitivity comparison of the suggested method with other previously reported methods

Table 6 compares the detection limit of the proposed method with UV-Vis spectrometry, spectrofluorimetry, RI, ICP-AES and potentiometric methods. As can be seen, the sensitivity of FFT-CCV method is better than most of them.

Table 6. Comparison between the detection limits of the proposed method with the other reported methods

Separation Method	Detection Method	Detection Limit	Ref.
IEC	Vis	~ 10 ppm	13
IEC	Vis	5 ppm	16
IEC	Spectrofluorimetry	(mg Scale)	17
IEC	Spectrofluorimetry	(mg Scale)	18
CE	UV	240 – 470 ppb	19
SPE-RP-Ion Pair-HPLC	UV, RI	10 ppm	20
IEC	ICP-AES	110 – 25 ppb	21
CE	UV	530 – 960 ppb	22
RP-HPLC	Diod Array Detector	> 9 ppm	23
CE	UV	4.8 ppm	24
IEC	Vis	25 ppm	39
-	Potentiometry	111 ppb	40
-	Potentiometry	113 ppb	45
-	Potentiometry	1 ppm	47
-	Potentiometry	90 ppb	48
HPCIC	Vis	4 ppm	58
IEC	FFT-CCV	90 ppb	This Work

ACKNOWLEDGEMENTS

The authors are grateful to the Research Council of University of Tehran for the financial support of this work.

References

1. M. R. Buchmeiser, *Rev. Anal. Chem.* 20 (2001) 161.
2. C. H. Knight, R. M. Cassidy, B. M. Recoskie and L. W. Green, *Anal. Chem.* 56 (1984) 474.
3. S.P. Verma, *Lanthan. Actin. Res.* 3 (1991) 237.
4. S.P. Verma, *Geostand. Newslett.* 15 (1991) 129.
5. Y. Inoue, H. Kumagai and Y. Shimimura, *Anal. Chem.* 68 (1996) 1517.
6. Ş. Kutun and A. Akseli, *J. Chromatogr. A*, 847 (1999) 261.

7. Ş. Kutun and A. Akseli, *J. Chromatogr. A*, 874 (2000) 311.
8. N. Öztekin and F. B. Erim, *J. Chromatogr. A*, 895 (2000) 263.
9. M. R. Buchmeiser, G. Seeber and R. Tessadri, *Anal. Chem.* 72 (2000) 2595.
10. N. Öztekin and F. B. Erim, *J. Chromatogr. A*, 924 (2001) 541.
11. N. M. Raut, P. G. Jaison and S. K. Aggarwal, *J. Chromatogr. A*, 1052 (2004) 131.
12. A. Mazzucotelli, A. Dadone, R. Frache and F. Baffi, *Chromatographia*, 15 (1982) 697.
13. P. N. Nesterenko and P. N. Jones, *J. Chromatogr. A*, 804 (1998) 223.
14. N. M. Raut, P. G. Jaison and S. K. Aggarwal, *J. Chromatogr. A*, 959 (2002) 163.
15. E. Santoyo, R. García, K. A. Galicia-Alanis, S. P. Verma, A. Aparicio and A. Santoyo-Castelazo, *J. Chromatogr. A*, 1149 (2007) 12.
16. E. A. Jones, H.S. Bezuidenhout and J. F. Van Staden, *J. Chromatogr.* 537 (1991) 277.
17. R. Kuroda, T. Wada, Y. Kokubo and K. Oguma, *Talanta*, 40 (1993) 237.
18. M. C. Bruzzoniti, E. Mentasti and C. Sarzanini, *Anal. Chim. Acta*, 353 (1997) 239.
19. G. J. Sevenich and J. S. Fritz, *Anal. Chem.* 55 (1983) 12.
20. A. W. Al-Shawi and R. Dahl, *Anal. Chim. Acta*, 333 (1996) 23.
21. E. H. Borai, M. A. Eid and H. F. Aly, *Anal. Bioanal. Chem.* 372 (2002) 537.
22. P. Jones and P. N. Nesterenko, *J. Chromatogr. A*, 789 (1997) 413.
23. C. Y. Liu, N. M. Lee and T. H. Wang, *Anal. Chim. Acta*, 337 (1997) 173.
24. P. Dufek, M. Vobecky, J. Holik and J. Valasek, *J. Chromatogr.* 435 (1988) 249.
25. S. Elchuk and R. M. Cassidy, *Anal. Chem.* 51 (1979) 1434.
26. R. M. Cassidy, S. Elchuk, N. L. Elliot, L. W. Green, C. H. Knight and B. M. Recoskie, *Anal. Chem.* 58 (1986) 1181.
27. D. J. Barkley, M. Blanchette, R. M. Cassidy and S. Elchuk, *Anal. Chem.* 58 (1986) 2222.
28. J. M. Hwang, J. S. Shih, Y. C. Yeh and S. C. Wu, *Analyst*, 106 (1981) 869.
29. S. Elchuk, K. I. Burns, R. M. Cassidy and C. A. Lucy, *J. Chromatogr.* 558 (1991) 197.
30. R. Kuroda, T. Wada, G. Kishimoto and K. Oguma, *Chromatographia*, 32 (1991) 65.
31. L. E. Vera-Avila and E. Camacho, *J. Liq. Chromatogr.* 15 (1992) 835.
32. R. G. Fernández and J. I. G. Alonso, *J. Chromatogr. A*, 1180 (2008) 59.
33. C. Nuryono, G. Huber and K. Kleboth, *Chromatographia*, 48 (1998) 407.
34. H. Z. Wu, N. Watanabe, Y. Gohshi and R. Kotama, *Fresenius J. Anal. Chem.* 363 (1999) 424.
35. K. Yoshida and H. Haraguchi, *Anal. Chem.* 56 (1984) 2580.
36. J. I. Garcia Alonso, F. Sena, Ph. Arbore, M. Betti and L. Koch, *J. Anal. At. Spectrom.* 10 (1995) 381.
37. B. A. Haley and G. P. Klinkhammer, *Mar. Chem.* 82 (2003) 197.
38. M. Vaughan and G. Horlick, *Appl. Spectrosc.* 40 (1986) 434.
39. S. H. Tan and G. Horlick, *Appl. Spectrosc.* 40 (1986) 445.
40. M. R. Ganjali, Z. Memari, F. Faridbod, R. Dinarvand and P. Norouzi, *Electroanalysis*, 20 (2008) 2663.
41. M. B., Saleh, A. A. A. Gaber, M. M. R., Khalaf and A. M., Tawfeek, *Anal. Lett.* 39 (2006) 17.
42. V. K. Gupta, A. K. Singh and B. Gupta, *Anal. Chim. Acta*, 575 (2006) 204.
43. H. A. Zamani and M. Mohaddeszadeh, *Anal. Lett.* 41 (2008) 2710.
44. M. R. Ganjali, S. Rasoolipour, M. Rezapour, P. Norouzi and M. Adib, *Electrochem. Commun.* 7 (2005) 989.
45. M. R. Ganjali, P. Norouzi, F. S. Mirnaghi, S. Riahi and F. Faridbod, *IEEE Sens. J.* 115 (2007) 1138.
46. F. Faridbod, M. R. Ganjali, R. Dinarvand, P. Norouzi and S. Riahi, *Sensors* 8 (2008) 1645.
47. H. A. Zamani, M. R. Ganjali, P. Norouzi and S. Meghdadi, *Anal. Lett.* 41 (2008) 902.
48. H. Behmadi, H. A. Zamani, M. R. Ganjali and P. Norouzi, *Electrochim. Acta*, 53 (2007) 1870.
49. M. R. Ganjali, P. Norouzi, A. Daftari, F. Faridbod and M. Salavati-Niasari, *Sens. Actuators B*, 120 (2007) 673.

50. M. R. Ganjali, M. Tavakoli, F. Faridbod, S. Riahi, P. Norouzi and M. Salavati-Niasari, *Int. J. Electrochem. Sci.* 3 (2008) 1559.
51. M. R. Ganjali, R. Nemati, F. Faridbod, P. Norouzi and F. Darviche, *Int. J. Electrochem. Sci.* 3 (2008) 1288.
52. M. R. Ganjali, F. Faridbod, P. Norouzi, and M. Adib, *Sens. Actuator B* 120 (2006) 119.
53. P. T. Kissinger and W. R. Heineman, *Laboratory Techniques in Electroanalytical Chemistry*, Marcel Dekker, New York, 1984.
54. L. Kristoffersen, A. Bugge, E. Lundanes and L. Slørdal, *J. Chromatogr. B*, 734 (1999) 229.
55. S. F. Y. Li, *Capillary Electrophoresis, Principles Practice and Applications*, Elsevier, Amsterdam, 1992.
56. R. M. Wightman and D. O. Wipf, in: A. J. Bard (Ed.), *Electroanalytical Chemistry*, vol. 15, Marcel Dekker, New York, 1989.
57. M. Paeschke, F. Dietrich, A. Ulig and R. Hintsche, *Electroanalysis*, 8 (1996) 891.
58. T. Dimitrakopoulos, P. W. Alexander and D. B. Hibbert, *Electroanalysis*, 8 (1996) 438.
59. R. Hintsche, M. Paeschke, U. Wollenberger, U. Schnakenberg, B. Wagner and T. Lisec, *Biosens. Bioelectron.* 9 (1994) 697.
60. V. Cosofret, M. Erdosy, T. A. Johnson, R. P. Buck, R. B. Ash and M. R. Neuman, *Anal. Chem.* 67 (1995) 1647.
61. A. S. Baranski, P. Norouzi and L. Nelsson, *J. Proc. Electrochem. Soc.* 96 (1996) 41.
62. CRC Handbook of Chemistry and Physics, 76th Edition, 1995.
63. P. Norouzi, M. R. Ganjali and P. Matloobi, *Electrochem. Commun.* 7 (2005) 33.
64. P. Norouzi, G. R. Nabi Bidhendi, M. R. Ganjali, A. Sepehri and M. Ghorbani, *Microchim. Acta* 152 (2005) 123.
65. M. R. Ganjali, P. Norouzi, M. Ghorbani and A. Sepehri, *Talanta*, 66 (2005) 1225.
66. P. Norouzi, M. R. Ganjali, M. Ghorbani and A. Sepehri, *Sens. Actuators B*, 110 (2005) 239.
67. P. Norouzi, M. R. Ganjali, T. Alizadeh and P. Daneshgar, *Electroanalysis* 18 (2006) 947.
68. J. Lipkowski and L. Stolberg, *Adsorption of Molecules at Metal Electrodes*, VCH, New York, 1992.
69. J. O. M. Bockris, B. E. Conway and E. Yeager, *Comprehensive Treatise of Electrochemistry*, Plenum, New York, London, 1980.
70. P. Norouzi, M. R. Ganjali, S. Shirvani-Arani and A. Mohammadi, *J. Pharm. Sci.* 96 (2007) 893.
71. P. Norouzi, S. Shirvani-Arani, P. Daneshgar and M. R. Ganjali, *Biosens. Bioelectron.* 22 (2007) 1068.
72. P. Norouzi, P. Daneshgar, M. R. Ganjali and A. A. Moosavi-Movahedi, *J. Brazilian Chem. Soc.* 18 (2007) 231.
73. P. Norouzi, M. R. Ganjali and P. Daneshgar, *Anal. Lett.* 40 (2007) 547.
74. P. Norouzi, M. R. Ganjali and L. Hajiaghababaei, *Anal. Lett.* 39 (2006) 1941.
75. P. Norouzi, M. R. Ganjali, S. Labbafi and A. Mohammadi, *Anal. Lett.* 40 (2007) 747.
76. P. Norouzi, M. R. Ganjali and P. Daneshgar, *J. Pharm. Toxicol. Method*, 55 (2007) 289.
77. S. P. Sinha, *Complexes of Rare-Earth*, 1st ed., Pergamon Oxford, London, 1966.
78. A. E. Martell and R. M. Smith, *Critical Stability Constants: Other Organic Ligands*, Vol. 3, Plenum, New York, 1977, p.28.
79. H. P. Fuping, P. R. Haddad, P. E. Jackson and J. Carnevale, *J. Chromatogr.* 640 (1993) 187.
80. A. Mohammadi, I. Haririan, N. Rezanour, L. Ghiasi and R. B. Walker, *J. Chromatogr. A*, 1116 (2006) 153.
81. A. Mohammadi, I. Kanfer, V. Sewram and R. B. Walker, *J. Chromatogr. B*, 824 (2005) 148.
82. A. Mohammadi, N. Rezanour, M. Ansari Dogahneh, F. Ghorbani Bidkorbeh, M. Hashem and R. B. Walker, *J. Chromatogr. B*, 846 (2007) 215.
83. United States Pharmacopoeia 28-NF 23, United States Pharmacopoeial Convention, INC., M.D. Rockville, 2748, 2005.

84. J. C. Miller and J. N. Miller, *Statistics for Analytical Chemistry*, vol. 22, Ellis Horwood, Chichester, 1984, p. 82.
85. Z. Al-Kurdi, T. Al-Jallad, A. Badwanamd and A. M. Y. Jaber, *Talanta* 50 (1999) 1089.
86. International Conference on Harmonization (ICH) Topic Q2 B: *Validation of Analytical Procedures: Methodology*, The European Agency for the Evaluation of Medicinal Products, Geneva, 1996.
87. Y. V. Heyden, A. Nijhuis, J. Smeyers-Verbeke, B. G. M. Vandeginste and D. L. Massaret, *J. Pharm. Biomed. Anal.* 24 (2001) 723.